Journal of Nanofluids
Vol. 12, pp. 1859–1867, 2023
(www.aspbs.com/jon)

ARTICLE

Experimental Investigation of Coefficient of Performance Enhancement (COP) in Ice Plant Using Brine-Based Metal Oxide Nanofluids

Sandipkumar B. Sonawane[1,*], Suyash Y. Pawar[1], Ali J. Chamkha[2], Vikram A. Kolhe[3], R. Kings Krishna Nagarajasingh[4], Kailas V. Chandratre[5], Hitendra Kumar Lature[6], Satish J. Suryawanshi[1], and J. Sunil[4]

[1] *Department of Mechanical Engineering, MVPS's KBT College of Engineering, Nashik, Maharashtra 422013, India*
[2] *Faculty of Engineering, Kuwait College of Science and Technology, Doha District 35004, Kuwait*
[3] *Department of Mechanical Engineering, Late G.N. Sapkal College of Engineering, Maharashtra 422213, India*
[4] *Department of Mechanical Engineering, Annai Vailankanni College of Engineering, Kanyakumari 629702, Tamil Nadu, India*
[5] *Department of Mechanical Engineering, KVN NSPS's LGM Institute of Engineering Education and Research, Nashik, Maharashtra 422013, India*
[6] *BYOS Scientific Lab, Aman Nagar, Mowa, Raipur Chhattisgarh 492007, India*

The research investigates brine-based metal oxide nanofluids to improve heat transfer and ice plant COP. The novelty of the study is in the use of stable nanofluids of ZnO, CuO, and Al_2O_3 prepared using surfactants and ultra-sonication to improve the performance of an ice plant working on the vapor compression refrigeration cycle. The study found that the COP of the ice plant was significantly enhanced using these nanofluids, with the greatest improvement of 27% observed for Al_2O_3 nanofluids at a particle volume concentration of 0.3%. The experiment also showed a reduction in compressor power consumption by 22% at the same concentration and temperature, indicating the potential use of these nanofluids in ice plant applications. The study further demonstrated that the COP improvement was more significant at a controlled temperature of 20 °C than at 25 °C.

KEYWORDS: Nano Fluids, Heat Transfer, Thermal Conductivity, COP Enhancement, Brine.

1. INTRODUCTION

Nanofluids refer to the distribution of nanoparticles which possess high thermal conductivity in a base fluid. Thermal systems often utilize a variety of fluids to facilitate heat transfer, including water, ethylene glycol, refrigerants, and lubricating oils. These fluids are commonly used due to their heat transfer properties and availability. Operating expenditure of the thermal systems of the ice plant, gearbox, compressor, and power pack mainly depends on the power consumption of the prime mover used in these thermal systems. The heat carrying capacity of the traditional thermal fluids (water, ethylene glycol, refrigerant, and lubricating oil) worked in the ice plant, gearbox, compressor, and power pack decides the power consumption of the prime mover. Using better heat transfer performance fluid from an economic point of view in the thermal industries is always desirable. Conventional heat transfer fluids are known to have lower thermal conductivity, which can negatively impact the efficiency of heat transfer. This is based on the ranking of thermal conductivity of various heat transfer fluids.[1] Heat transfer and thermal conductivity performance of the convectional fluids can enhance by dispersing high thermal conductivity nanoparticles in them.[2–12]

The prime mover of the gearbox, compressor, power pack, and blower can use less energy if the efficiency of heat transfer of the conventional fluids is increased. There has been a great deal of study in recent years devoted to elucidating the specific heat, thermal conductivity, and viscosity of nanofluids. These properties, which can be used to enhance heat transfer performance in a variety of contexts, have been the subject of extensive research. This article provides a review of current experimental efforts. In the turbulent domain and with constant heat flux boundary conditions, Hamid et al.[13] evaluated the ability of a mixture of water, TiO_2 nanoparticles and ethylene glycol to transfer heat in convection mode. The

*Author to whom correspondence should be addressed.
Email: sonawane.sandipkumar@kbtcoe.org
Received: 7 March 2022
Accepted: 19 April 2023

study aimed to determine the performance of this mixture as a heat transfer fluid. Elcioglu et al.[14] investigated trial characteristics' effects on viscosity of nanofluids and relative viscosity using the Taguchi Method. Nanofluids were analysed, and it was found that the correlation between temperature and particle concentration had a significant impact on the nanofluids' viscosity. The fluid's thermal performance, such as its heat transfer rate and efficiency, depends heavily on this correlation. The fluid's viscosity is a crucial variable because it affects both the fluid's flow rate and its capacity to transfer heat within the system. Optimizing the heat transfer performance of the nanofluids requires knowledge of the interplay between temperature, particle concentration, and viscosity, as shown by the present research. Kumar et al.[15] evaluated the nanofluids heat transfer characteristics of heat exchangers by considering various factors (base fluid, pressure difference, sonication time, temperature) and obtained 28%, 26% and 25% enhancements in the convective heat transfer coefficient using Al_2O_3–paraffin, Al_2O_3-EG nanofluids and Al_2O_3–water nanofluid respectively at a particle concentration of 0.08 by volume percentage. Hamid et al.[16] conducted an experimental study to examine the thermophysical properties of a nanofluids made from a mixture of ethylene glycol (20:80) and TiO_2–SiO_2 nanoparticles. They found that nanofluids had a thermal conductivity that was 16% higher than that of water alone. Akilu et al.[17] found no effect on base liquid electrical conductivity and pH with a temperature change. However, they observed that nanofluids thermal and electrical conductivity significantly increased with an increase in temperature. Water-based ZnO–Ag nanofluids was developed by Esfahani et al.[18] using a two-stage procedure, a magnetic mixture, an ultrasonic device, and acidity control methodology. They obtained a 2% rise in relative thermal conductivity at 50 °C and particle volume fraction of 2%. A summary of numerical and experimentation studies of thermal performance and thermo-physical properties of glycol-based nanofluids has been proposed by Sekrani and Poncet.[19]

The study conducted by Ambreen and Kim[20] involved a comparison of heat transfer correlations for nanofluids in relation to the flow conditions, boundary conditions, and geometrical configurations of the system. Yu et al.[21] reviewed the efforts and progress in improving thermal nanofluids dispersion stability. Bi et al.[22] carried out experimental evaluation of the reliability and thermal performance of a household refrigerator using nanoparticles. They have obtained 26.1% less energy consumption using HFC134a and POE-based TiO_2 nanofluids at a 0.1% mass fraction. Bi et al.[23] conducted an experimental research on R600a + TiO_2 nanofluids for domestic refrigerators and obtained approximately 9.6% energy savings. Vallejo et al.[24] have reviewed the empirical studies on hybrid and mono nanofluids for practical uses such as tubular and plate heat exchangers, heat sink/mini channel heat exchangers and heat pipe.

Okonkwo et al.[25] conducted a comprehensive review of nanofluids synthesis, thermo physical property measurement, and nanofluids applications for thermal devices (solar collectors, thermal storage, heat exchangers and electronics cooling. They have also reviewed the enhanced thermal behavior of nanofluids. Gorla et al.[26] investigated heat transfer and flow of a Cu–Al_2O_3–water hybrid nanofluid through a square porous cavity. The heat source and sink location, nanoparticle volume fraction, and Hartmann number significantly affect fluid flow and heat transfer inside the cavity. The study has major implications for nanofluid heat transfer system design. Mansour et al.[27] examined entropy generation, magneto-hydrodynamics, natural convection flow, and heat transfer. The left and right cavity walls were cooled, while the top and bottom were heated. The finite difference method solved the governing equations numerically using nanofluid thermal conductivity and dynamic viscosity data. Entropy production was examined in relation to the Hartmann number, nanoparticle volume fraction, cavity geometric parameters, and other studies.

Several studies on the impact of using nanoparticles are referenced [28–34] in the study. According to the results of the aforementioned studies, fluid velocities decrease with increasing rotation, while Hall slip parameter, ion slip parameter, and dufour parameter all increase velocities. The radiation-absorption parameter was observed to increase the thermal boundary layer thickness, whereas the suction parameter was found to decrease the Nusselt number. Additionally, the chemical reaction parameter was found to increase the Sherwood number. Brine is chosen as a base fluid for this research study due to its potential heat transfer application in the ice plant. It is used as a secondary refrigerant in the ice plant. The literature does not contain studies on the synthesis or Coefficient of performance (COP) of brine-based metal oxide nanofluids used in ice plants. COP of the ice plant is the ratio of refrigerating effect produced to the compressor power consumption. It is suggested that metal oxide nanoparticles (ZnO, CuO, and Al_2O_3) be suspended in brine to improve the COP of the ice plant. In the current experimental study, stable brine-based nanofluids with metal oxide nanoparticles (ZnO, CuO and Al_2O_3) are prepared and evaluated for the COP of the ice plant. The effects of particle volume fraction, surrounding temperature and material on the COP of the ice plant are experimentally investigated in this research work. These experimental findings identified the best brine-based metal oxide nanofluids for future use in ice plants.

2. SYNTHESIS OF NANOFLUIDS

Synthesis of nanofluids is the first important step in nanofluids research. For the preparation of brine, 30%

of ethylene glycol is mixed with 70% of distilled water on a volume basis. Brine-based nanofluids with metal oxide nanoparticles (ZnO, CuO, Al_2O_3) prepared at particle volume fractions of 0.05%, 0.1%, 0.2% and 0.3%. ZnO, CuO and Al_2O_3 nano-particles of average particle size of 30 nm were utilized (Supplier: Nanostructured & Amorphous Materials, Inc., USA). Transmission Electron Microscope (TEM) images of ZnO, CuO and Al_2O_3 nano-particles are shown in Figures 1–3, respectively. Oleic acid and CTAB are used as the surfactants to prepare stable brine-based metal oxide nanofluids to avoid the agglomeration issue raised because of strong forces of attraction (Van Der Waals forces) of nanoparticles.[35] Sonawane et al.[10] describe the procedure that used to produce the nanofluids.

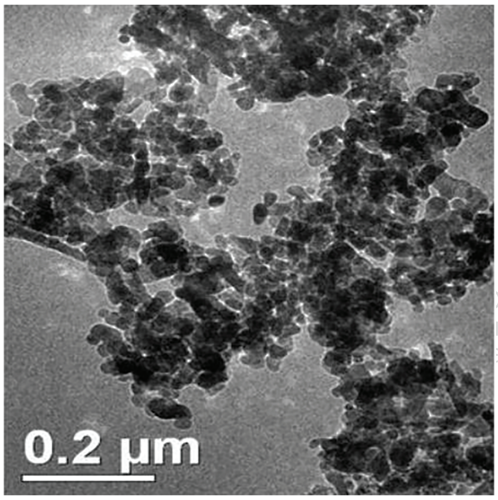

Fig. 1. TEM image of ZnO nanoparticles.

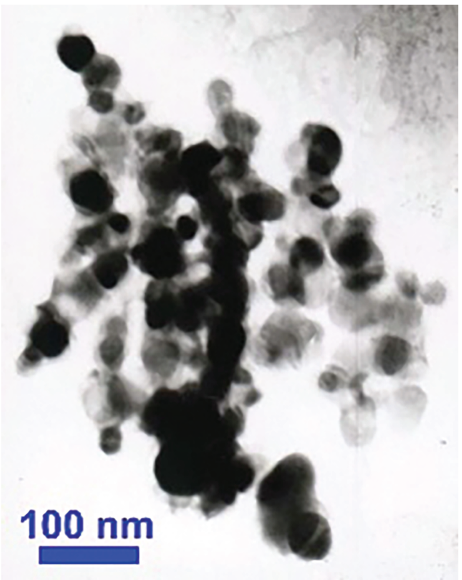

Fig. 2. TEM image of CuO nano-particles.

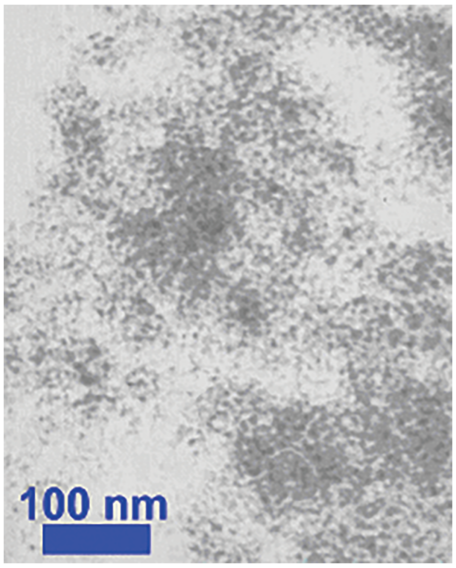

Fig. 3. TEM image of Al_2O_3 nano-particles.

Various tests investigated the exact concentration of surfactants used in brine to prepare stable nanofluids. The brine-based stable ZnO, CuO, and Al_2O_3 nanofluids have been made using the right concentration of surfactants and an ultra-sonication technique. Table I shows the surfactant concentration, ultra sonication time, and period of stable suspension of brine-based metal oxide nanofluids.

3. EXPERIMENTAL SET-UP

In this study, the COP of a brine-based metal oxide nanofluid ice plant was measured using an experimental setup. A condenser, compressor, evaporator, expansion valve, and receiver made up the vapor compression refrigeration cycle used in this method. The primary refrigerant vapor (R22) was heated and pressurized by the compressor after leaving the evaporator. After passing through the forced air-cooled condenser, the high-pressure, high-temperature refrigerant vapor became a liquid, which was collected in the receiver. The primary refrigerant was then expanded from high pressure to low pressure using a capillary tube (expansion device). The experimental set-up shown in Figure 4 was used to conduct the experiments and measure the COP of the ice plant. The set-up included all the components of the refrigeration cycle mentioned above. The experiments were conducted by adding stable nanofluids of ZnO, CuO, and Al_2O_3 prepared using surfactants and ultra-sonication, to the brine solution. The COP was then determined for each nanofluid at different particle volume concentrations and temperatures. The experiment was conducted under controlled laboratory conditions to ensure accuracy and reliability of the results.

Low pressure and low-temperature refrigerant from the capillary tube (shown in Fig. 4) vaporized by the heat

Table I. Synthesis of brine-based metal oxide nanofluids.

Nano fluids	The volume of brine in ml	Ultra sonication time in hrs	Oleic acid in ml	CTAB in gms	Period of stable suspension after sonication in hrs
Brine + 0.05% ZnO	1000	3	3.8	1	6
Brine + 0.1% ZnO	1000	3	3.8	2	6
Brine + 0.2% ZnO	1000	3	3.8	3	6
Brine + 0.3% ZnO	1000	3	3.8	4	6
Brine + 0.05% CuO	1000	2	3.46	–	6
Brine + 0.1% CuO	1000	2	3.46	–	6
Brine + 0.2% CuO	1000	2	3.46	–	6
Brine + 0.3% CuO	1000	2	3.46	–	6
Brine + 0.05% Al_2O_3	1000	5	3.46	–	6
Brine + 0.1% Al_2O_3	1000	5	3.46	–	6
Brine + 0.2% Al_2O_3	1000	5	3.46	–	6
Brine + 0.3% Al_2O_3	1000	5	3.46	–	6

from the brine (stored in the insulated brine/nanofluids tank). Hence brine gets cooled. This cooled brine further absorbs the heat from water (filled in the ice cans), and the phase transforms from water to ice. These ice cans have been soaked in a brine solution. Hence the heat transfer occurs from water (available in the ice can) to brine across the walls of the ice cans. Temperatures of the primary (R22) and secondary refrigerant (brine) at various locations are measured using thermocouples. The initial temperature of the water was kept at 25 °C, and ice formed at −2 °C for all the experimental trials. Initially, the practice tests were conducted using brine as a secondary refrigerant. Then brine is removed from the brine tank and replaced with brine-based metal oxide nanofluids. Primary refrigerant (R22) is kept the same in both cases. Compressor power consumption is measured by an energy meter. Experimental readings of temperature, pressure and the energy meter were transmitted to the computer through Labview software. Refrigerating effect and electrical power required to drive the refrigerating compressor for the production of ice are determined using the experimental data stored in the computer. Equations used to evaluate the COP of the ice plant are described in the next section.

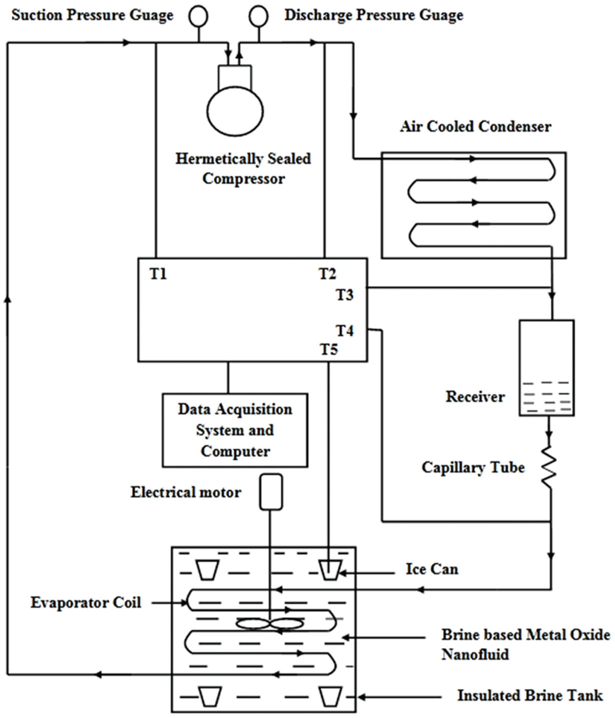

Fig. 4. Illustrative diagram of the experimental set-up used for measurement of COP using brine-based metal oxide nanofluids.

The procedure used for the calculation of COP using experimental data is as follows.[36] Refrigerating effect (RE) of the ice plant can obtain using equation,

$$\text{RE} = \text{Water's sensible heat} + \text{Latent heat of ice} + \text{Ice's sensible Heat}$$

$$\text{The Water's sensible heat} = m \times C_p \times \Delta T \qquad (1)$$

Where m, C_p and ΔT are the mass of water filled in ice cans (kg), the specific heat of water (kJ/kg K) and the difference between the initial temperature of water (25 °C) and freezing point of water (0 °C) respectively.

$$\text{Latent heat of ice} = m \times h_{fg} \qquad (2)$$

$$\text{The sensible heat of ice} = m \times C_{pice} \times \Delta T \qquad (3)$$

where m, h_{fg} and ΔT are the mass of ice produced in the ice cans (kg), latent heat of ice (335 kJ/kg) and temperature difference of ice (2 °C), respectively. All the experimental trials recorded the time (t) required for ice formation at −2 °C from water at 25 °C.

Compressor power consumption (kWh) is determined using,

$$E = E_1 - E_2 \qquad (4)$$

Where E_1 = Energy meter reading at which ice gets formed at −2 °C Temperature.

E_2 = Energy meter reading at the beginning of the trial (at 25 °C of water kept in ice cans).

Several assumptions were made in the calculation of the Coefficient of Performance (COP) of an ice plant operating on a simple saturated vapor compression cycle. To begin, the cycle was assumed to have isentropic compression, constant pressure condensation, is enthalpic, and constant pressure evaporation processes. In a simple saturated vapor compression cycle, it was also assumed that the refrigerant was dry saturated vapor before compression and saturated liquid after condensation. Furthermore, in this cycle, the refrigerant was assumed to be an ideal working fluid. These assumptions were made to simplify the COP calculation and obtain accurate results. The heat transfer between the refrigerant and its surroundings was also assumed to be negligible. This assumption was made to simplify the COP calculation and ensure that heat transfer from the system had no effect on the accuracy of the results.[37] The COP of an ice plant operating on a simple saturated vapor compression cycle (shown in Fig. 5) is calculated using Eq. (5).

$$(\mathrm{COP})_{\mathrm{ideal}} = \frac{h_1 - h_4}{h_2 - h_1} \tag{5}$$

where h_1, h_2, h_4 = Enthalpy of refrigerant before compression, after compression and Enthalpy of refrigerant before evaporation respectively.

The value of experimental COP of the ice plant is measured using,

$$(\mathrm{COP})_{\mathrm{Experimental}} = \frac{\text{Refrigerating effect}}{\text{Compressor power}} \tag{6}$$

The refrigerating effect obtained from Eqs. (1)–(3), whereas compressor power is determined using Eq. (4).

Percentage enhancement in the COP can be determined using

$$\text{Percentage enhancement} = \frac{(\mathrm{COP})_{\mathrm{NR}}}{(\mathrm{COP})_{\mathrm{brine}}} \times 100 \tag{7}$$

where $\mathrm{COP}_{\mathrm{NR}}$ = COP of the ice plant using brine-based metal oxide nanofluids as a secondary refrigerant.

$\mathrm{COP}_{\mathrm{brine}}$ = COP of the ice plant using brine as a secondary refrigerant.

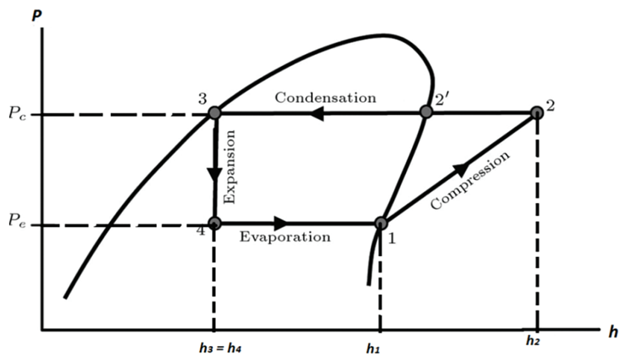

Fig. 5. Simple saturated vapor compression cycle on $p-h$ diagram.

4. NANOPARTICLE DEPOSITION IN EXPERIMENTAL SETUP

The present work confirmed the repeatability of experimental data by measuring the COP of brine + 0.3% Al_2O_3 nanofluids four times for two months. Based on repeated experimental results, it was concluded that the chances of nanoparticle accumulation, deposition, and coating when nanofluids is in motion were relatively low. Also, when the nanofluids were kept stagnant in a brine tank, the nanoparticles started settling after the period of stable suspension (mentioned in Table I). However, the nanofluids regained stability if stirred for a few minutes in the brine tank and remained stable for approximately the period of stable suspension.

5. EXPERIMENTAL RESULTS AND DISCUSSION

After the validation of the experimental set-up, trials have been conducted on a computerized experimental set-up of an ice plant using brine (30% of ethylene glycol mixed with 70% of distilled water on a volume basis) as a secondary refrigerant and the COP of the ice plant measured for this case. Then COP of the ice plant is measured using brine-based nanofluids (secondary refrigerant) with metal oxide nanoparticles (ZnO, CuO and Al_2O_3) at 0.05%, 0.1%, 0.2% and 0.3% particle volume fractions respectively. R22 is used as the primary refrigerant in both cases, and experimental trials were carried out at a controlled surrounding temperature of 25 °C. R22 is used as the primary refrigerant in both cases. Practical tests were carried out at a steady surrounding temperature of 25 °C. The initial temperature of the water was 25 °C, and the temperature of ice produced was −2 °C, kept the same for all the experimental trials. The surrounding temperature of the cabinet (at which the experimental set-up is held) is maintained at 25 °C using the split air conditioner. Experimental values of the COP of the ice plant are plotted against the particle volume concentrations of metal oxide nanoparticles (ZnO, CuO and Al_2O_3) in Figure 6.

It has been seen from Figure 6 that the COP of brine-based metal oxide nanofluids improved with rise in the particle volume concentration. Experimentally measured values of COP compared with the ideal values at different particle volume concentrations. Ideal values of COP are approximately 17% more than experimental COP at a particular particle volume concentration. The thermodynamic processes in actual VCC involve irreversibility, which causes frictional and heat losses. Also, refrigerant vapour condition is assumed to be dry and saturated at the beginning of compression, whereas it is the dry saturated liquid after the condensation process. These conditions are not available in an experimental cycle. As a result, experimental values of COP are less than ideal one. However, qualitatively excellent COP values show good agreement with the experimental one. Percentage

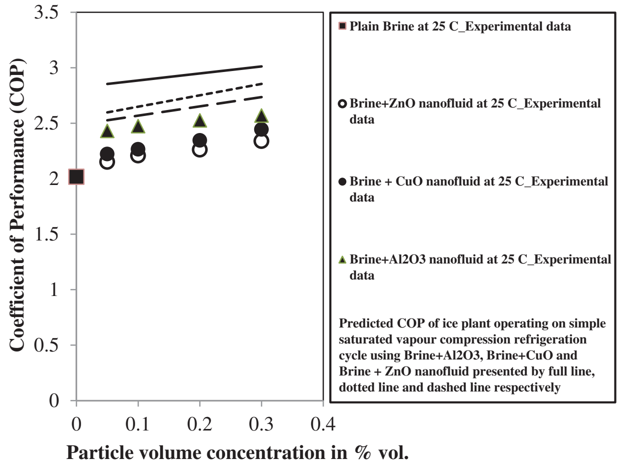

Fig. 6. Effect of concentration volume and material on COP of brine-based metal oxide nanofluids.

enhancement in the COP is determined using the procedure described in Section 4. Figure 7 presents these results (percentage enhancement in the COP) at various volume concentrations of particles. It has been seen from Figure 7 that percentage enhancement in the COP increases with a rise in particle volume concentration. Also, a comparison among the three metal oxides indicates that the improvement in the COP is more significant for the brine–Al_2O_3 nanofluids for all particle volume concentrations. In particular, the brine–Al_2O_3, brine–CuO, and brine–ZnO nanofluids show enhancement in the COP by 27%, 19% and 15% respectively at 0.3% particle concentration by volume. Enhancement in the COP is correlated to the thermal conductivity of metal oxide nanoparticles (ZnO, CuO and Al_2O_3). It has been seen clearly that nanoparticles with higher thermal conductivity exhibit better COP of nanofluids at all particle volume concentrations. The phenomenon known as "micro-convection" effect, which describes the synergistic relationship between the base fluid molecules and nanoparticles, is believed to be primarily responsible for the improvement in thermal conductivity. This effect is caused by the movement of high thermal conductivity nanoparticles on the outer surface of the copper tube, which increases the near-wall temperature gradient. The utilization of nanofluids results in higher coefficient of performance (COP) values due to the decrease in thermal boundary layer thickness and increase in heat transfer rate from the brine to the primary refrigerant. Additionally, it also leads to enhancement of the particle volume concentration.

From an engineering estimation point of view, compressor power required for the production of unit Ton of refrigeration using brine-based metal oxide nanofluids is studied experimentally, and results are presented in Figure 8. It has been clearly analysed that compressor power consumption of nanofluids is lower compared with the simple brine. Also, compressor power consumption decreases with an particle volume concentration increment. In particular, maximum saving of compressor power of approximately 21% is obtained using brine–Al_2O_3 nanofluids at 0.3% volume concentration of particle in comparison with the simple brine. It indicates that brine–Al_2O_3 nanofluids is the most suitable nanofluids for ice plant application. To assess the economic viability of nanofluids in various HVAC applications, the viscosity of brine/nanofluids must be measured from the standpoint of pumping power. The viscosity (dynamic) of metal based oxide nanofluids, specifically those based on brine was measured at varying particle concentrations by volume of 0.05%–0.3% and at a 25 °C constant temperature.

Figure 9 displays the collected data as a function of particle volume concentration; the dynamic viscosity of plain brine at zero particle volume concentration is also shown for comparison. According to the results, the dynamic viscosity of nanofluids rises with increasing volume concentration. In addition, when compared to other metal oxide nanofluids like brine–CuO and brine–Al_2O_3 nanofluids, brine–ZnO nanofluids showed the highest dynamic viscosity values at the same particle volume concentration. Figure 10 shows how the particle concentration in a given volume causes the nanofluids' dynamic viscosity to rise. The dynamic viscosity is seen to rise linearly with particle concentration in volume. In particular, at a volume concentration of particle of 0.3% and 25 °C, brine–ZnO nanofluids showed a 15% increase in dynamic viscosity, whereas the brine–Al_2O_3 and brine-CuO nanofluids showed a

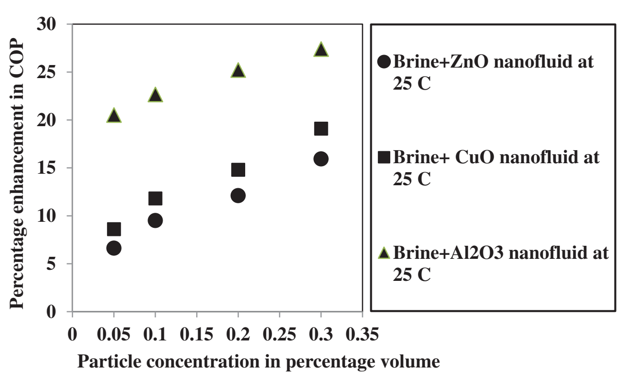

Fig. 7. Experimental results of percentage enhancement in the COP.

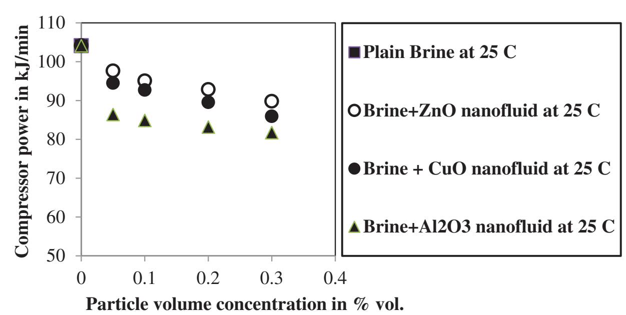

Fig. 8. Experimental results of compressor power consumption.

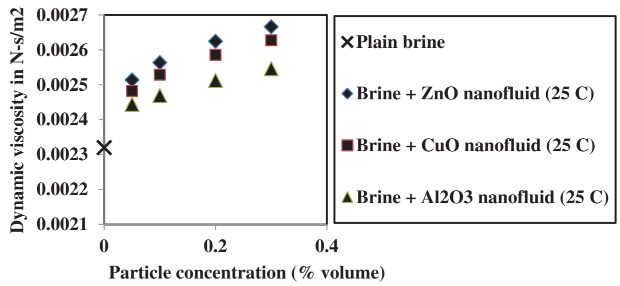

Fig. 9. Dynamic viscosity of Brine based metal oxide nanofluids as a function of volume concentration of particle.

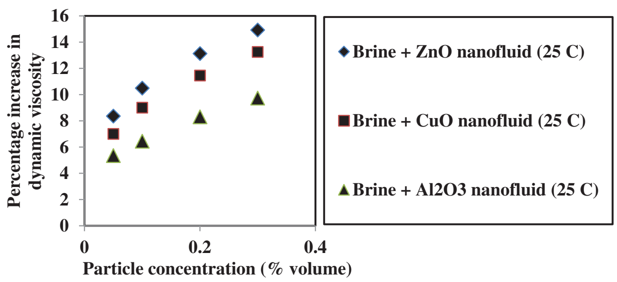

Fig. 10. Percentage rise in dynamic viscosity of Brine based metal oxide nanofluids as a function of particle volume concentration.

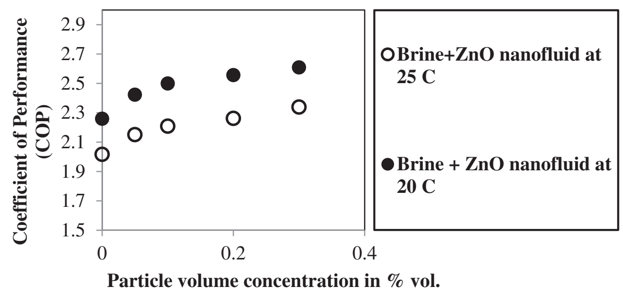

Fig. 11. Effect of surrounding temperature on COP of Brine–ZnO nanofluids.

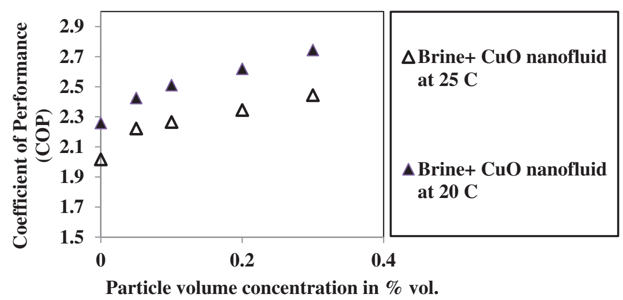

Fig. 12. Effect of surrounding temperature on COP of Brine–CuO nanofluids.

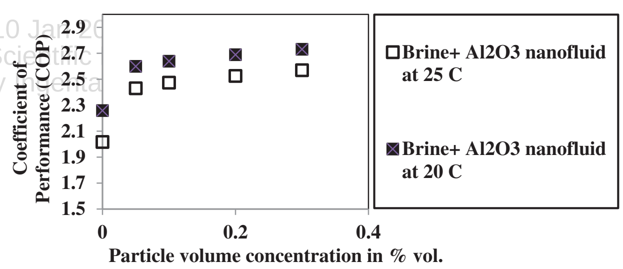

Fig. 13. Effect of surrounding temperature on COP of Brine–Al_2O_3 nanofluids.

10% and 13% increase in dynamic viscosity, respectively. The analysis of the data presented in Figures 7 and 9 reveals that the brine-based Al_2O_3 nanofluids exhibits better enhancement in coefficient of performance (COP) with a relatively lower increase in viscosity, making it a technically and economically viable option for heating, ventilation, and air conditioning (HVAC) applications.

The temperature effect on the COP of the brine-based metal oxide nanofluids (ZnO, CuO and Al_2O_3) at various particle volume concentrations (0.05% to 0.3%) is studied under controlled surrounding temperatures of 20 °C and 25 °C. Experimental results of the effect of surrounding temperature on the COP of the brine-based metal oxide nanofluids are presented in Figures 11–13. It has been observed that the COP of brine-based metal oxide nanofluids is higher at 20 °C surrounding temperature than 25 °C at all the particle volume concentrations. The power required to drive the compressor at 25 °C surrounding temperature is more significant than that needed at 20 °C, for obtaining an equal refrigerating effect/cooling effect. This can be explained using COP of the Carnot refrigerator (ideal refrigerator). COP of Carnot refrigerator is determined using

$$\mathrm{COP} = \frac{T_a}{T_b - T_a} \tag{8}$$

where T_a = temperature to be maintained in the refrigerator

T_b = temperature of the surroundings to which the heat rejected.

The evaporator temperature of the ice plant refrigeration system has been kept constant in all experimental trials. However, the temperature of the surrounding environment (to which the heat is rejected) was varied to investigate the temperature effect on the COP of the ice plant using brine-based ZnO, CuO, and Al_2O_3 nanofluids. According to Eq. (7), the COP of the Carnot refrigerator at 20 °C is greater than that at 25 °C at a constant value of T_a in all cases.

The novelty of the work is the experimental investigation of COP enhancement using brine based metal oxide nanofluids (ZnO, CuO, and Al_2O_3) in an ice plant. Using brine-based nanofluids of varying particle volume fractions, the COP of the ice plant was measured, and it was found that the COP increased with increasing particle volume concentration. Brine–Al_2O_3 nanofluids showed the greatest COP improvement. Metal oxide nanoparticles' high thermal conductivity was linked to their improved COP. Nanofluids improved COP because they facilitated greater heat transfer from the brine to the primary refrigerant and consequently reduced the thickness of the thermal boundary layer. Nanofluids particle volume concentration-dependent reduction in compressor power consumption compared favorably to that of plain brine.[38–41]

6. CONCLUSIONS AND FUTURE SCOPE

1. The COP (Coefficient of Performance) of an ice plant was measured in this study using brine-based nanofluids containing metal oxide nanoparticles (ZnO, CuO, and Al_2O_3).
2. The effects of the volume concentration of particles, particle material, and surrounding temperature on the COP of the ice plant were experimentally investigated.
3. The experimental results showed that the COP enhancements for brine–Al_2O_3, brine–CuO, and brine–ZnO nanofluids were 27%, 19%, and 15%, respectively, at 0.3% volume concentration of particles.
4. The increase in temperature gradient close to the wall due to the migration of nanoparticles with high thermal conductivity is responsible for the enhancement of heat transfer and hence better COP.
5. The COP of brine-based Al_2O_3, CuO, and ZnO nanofluids was found to be more significant at 20 °C of surrounding controlled temperature than that of 25 °C at 0.3% volume concentration of particles.
6. The experimental results demonstrate that brine-based ZnO, CuO, and Al_2O_3 nanofluids are suitable for better heat transfer as a secondary refrigerant in ice plant applications.
7. Among the investigated nanofluids, brine–Al_2O_3 was found to be the most suitable energy-efficient nanofluid that can be used as a secondary refrigerant in ice plant applications and other HVAC applications.

Due to their heat transfer enhancement, nanofluids are increasingly used in refrigeration and lubrication. There are contradictions in research findings, and more studies are needed to understand nanofluid thermo physical properties, surface tension, and dielectric properties. Research is also needed on hybrid nanofluids, natural refrigerant-based nanofluids, brine-based nanofluids, and low-temperature nanofluids. The cooling tower/condenser circuit and nanofluid crystallizations phase change characteristics need research. Improved energy storage systems require nano phase change materials (nano PCM) and nano enhanced phase change materials (NePCM). In order to optimize their use in ice plants, this study suggests studying the long-term stability, economic feasibility, and performance of brine-based metal oxide nanofluids.

Acknowledgments: The authors would like to extend their gratitude to the Science and Engineering Research Board, Department of Science and Technology, Government of India (File No. YSS/2014/000759) for funding this research study.

NOMENCLATURE

Abbreviations

COP Coefficient of Performance
TEM Transmission Electron Microscope
Cu Copper
Al_2O_3 Aluminum Oxide
CuO Copper Oxide
ZnO Zinc Oxide
CTAB Cetyl Trimethyl Ammonium Bromide
RE Refrigerating effect

Symbols

m Mass
C_p Specific heat
h_{fg} Latent heat of ice
h Enthalpy
ΔT Temperature difference

Greek Symbol

μ Dynamic viscosity

References and Notes

1. S. Choi, ASME *Publications* 231/66, 99 (**1995**).
2. D. Madhesh and S. Kalaiselvam, *Procedia Engineering* 97, 1667 (**2014**).
3. A. Nayak, M. Garcia, and P. Vijayan, *Exp. Therm. Fluid Sci.* 33, 184 (**2008**).
4. S. Thomas, K. S. Kumar, and C. Sobhan, *Advanced Materials Research* 685, 145 (**2013**).
5. S. Peyghambarzadeh, S. Hashemabadi, S. Hoseini, and M. Seifi Jamnani, *International Communications in Heat and Mass Transfer* 38, 1283 (**2011**).
6. A. Iam and R. Saider, *Appl. Therm. Eng.* 32, 76 (**2012**).
7. D. Agarwal, A. Vaidyanathan, and S. Sunil Kumar, *Appl. Therm. Eng.* 60, 275 (**2013**).
8. M. Chandrasekar, S. Suresh, and A. Chandra Bose, *Exp. Therm. Fluid Sci.* 34, 210 (**2010**).
9. W. Duangthongsuk and S. Wongwises, *Exp. Therm. Fluid Sci.* 33, 706 (**2009**).
10. S. K. Sonawane, K. Patankar, A. Fogla, U. Bhandarkar, B. Puranik, and S. Sunil Kumar, *Appl. Therm. Eng.* 31, 2841 (**2011**).
11. S. K. Sonawane, U. Bhandarkar, B. Puranik, and S. S. Kumar, *J. Thermophys. Heat Transfer* 26, 619 (**2012**).
12. S. K. Sonawane, U. Bhandarkar, and B. Puranik, *Journal of Thermal Science and Engineering Applications* 8, 031001 (**2016**).
13. K. A. Hamid, W. H. Azmi, R. Mamat, K. V. Sharma, and K. Abdul Hamid, *International Communications in Heat and Mass Transfer* 73, 16 (**2016**).
14. E. B. Elcioglu, A. G. Yazicioglu, A. Turgut, and A. S. Anagun, *Appl. Therm. Eng.* 128, 973 (**2018**).
15. N. Kumar, S. S. Sonawane, and S. H. Sonawane, *International Communications in Heat and Mass Transfer* 90, 1 (**2018**).
16. K. A. Hamid, W. H. Azmi, M. F. Nabil, R. Mamat, and K. V. Sharma, *Int. J. Heat Mass Transfer* 116, 1143 (**2018**).
17. S. Akilu, K. V. Sharma, A. T. Ba, M. S. M. Azman, and P. T. Bhaskoro, *Temperature Dependent Properties of Silicon Carbide Nanofluids in Binary Mixtures of Glycol* 148, 774 (**2016**).
18. N. N. Esfahani, D. Toghraie, and M. Afraid, *Powder Technol.* 323, 367 (**2018**).
19. G. Sekrani and S. Poncet, *Applied Sciences* 8, 2311 (**2018**).

20. T. Ambreen and M. H. Kim, *Renewable and Sustainable Energy Reviews* 91, 564 (**2018**).
21. F. Yu, Y. Chen, X. Liang, J. Xu, C. Lee, Q. Liang, P. Tao, and T. Deng, *Progress in Natural Science: Materials International* 27, 531 (**2017**).
22. S. S. Bi, L. Shi, and L. L. Zhang, *Appl. Therm. Eng.* 28, 774 (**2008**).
23. S. Bi, K. Guo, Z. Liu, and J. Wu, *Energy Convers. Manage.* 52, 733 (**2011**).
24. J. Vallejo, J. Prado, and L. Lugo, *Appl. Therm. Eng.* 203, 117926 (**2022**).
25. E. C. Okonkwo, I. Wole-Osho, I. W. Almanassra, Y. M. Abdullatif, and T. Al-Ansari, *J. Therm. Anal. Calorim.* 145, 2817 (**2021**).
26. R. S. Gorla, S. Siddiqa, M. A. Mansour, A. M. Rashad, and T. Salah, *J. Thermophys. Heat Transfer* 31, 847 (**2017**).
27. M. A. Mansour, S. Siddiqa, R. S. Gorla, and A. M. Rashad, *Thermal Science and Engineering* 6, 57 (**2017**).
28. Z. A. Abdelnour, A. Aissa, F. Mebarek-oudina, A. M. Rashad, H. M. Ali, M. Sahnoun, and M. El Ganaoui, *J. Therm. Anal. Calorim.* 141, 1981 (**2020**).
29. E. R. El-Zahar, A. M. Rashad, W. Saad, and L. F. Seddek, *Sci. Rep.* 10, 10494 (**2020**).
30. S. Jakeer, P. BalaAnki Reddy, A. M. Rashad, and H. A. Nabwey, *Alexandria Engineering Journal* 60, 821 (**2020**).
31. E. R. El-Zahar, A. E. Mahdy, A. M. Rashad, W. Saad, and L. F. Seddek, *Fluids* 6, 197 (**2021**).
32. A. Mourad, A. Aissa, F. Mebarek-Oudina, W. Jamshed, W. K. Ahmed, H. M. Ali, and A. M. Rashad, *International Communications in Heat and Mass Transfer* 126, 105461 (**2021**).
33. T. H. Alarabi, A. M. Rashad, and A. E. Mahdy, *Coatings* 11, 1490 (**2021**).
34. J. H. Shaik, B. A. Polu, M. Mohamed Ahmed, and R. Ahmed Mohamed, *The European Physical Journal Plus* 137, 1 (**2022**).
35. G. Cao, *Nanostructures and Nanomaterials*. London, Imperial College Press (**2004**).
36. B. Whitman, B. Johnson, J. Tomczyk, and E. Silberstein, *Refrigeration and air Conditioning Technology*. Cengage Learning, Boston, Massachusetts, United States (**2012**).
37. M. Prasad, *Refrigeration and Air Conditioning*. Willey Eastern Ltd., Mumbai, India (**1983**).
38. X. Zhang, P. Wu, L. Qiu, X. Zhang, and X. Tian, *Energy Convers. Manage.* 51, 130 (**2010**).
39. N. E. Wijeysundera, M. N. A. Hawlader, C. W. B. Andy, and M. K. Hossain, *International Journal of Refrigeration* 27, 511 (**2004**).
40. Y. Oda, M. Okada, S. Nakagawa, K. Matsumoto, and T. Kawagoe, *International Journal of Refrigeration* 27, 353 (**2004**).
41. Q. B. He, W. M. Tong, and Y. D. Liu, *International Journal of Refrigeration* 28, 33 (**2007**).

ARTICLE